Investigation of brain functional connectivity by resting-state fMRI in cerebral small vessel diseases

Maria do Carmo Cardoso de Menezes Moser, *Biomedical Engineering, Instituto Superior Técnico*

Abstract **- Resting-state functional magnetic resonance imaging (fMRI) studies have been a promising tool to assess functional connectivity (FC) for a variety of neurological and psychiatric disorders. However, few investigations include subjects with sporadic small vessel disease (S-SVD) and those with cerebral autosomal dominant arteriopathy with subcortical infarcts and leukoencephalopathy (CADASIL). The present work aims to investigate changes in brain FC measured by resting-state fMRI in these groups of patients compared with a healthy control group. For each subject, previously acquired structural images and resting-state fMRI data were pre-processed and subjected to group statistical analyses. Two distinct methods were used to assess functional connectivity (FC) differences between groups: a data-driven method, independent component analysis, and a model-based method, seed-based correlational analysis, focusing on three seeds, posterior cingulate cortex (PCC), supplementary motor area (SMA) and intraparietal sulcus (IPS). We found a significant increase in the FC of PCC, and a significant decrease in the FC of SMA and IPS, in both S-SVD and CADASIL relative to controls. Finally, a statistical analysis was conducted to assess whether demographical, neuropsychological and brain structure measures were correlated with the FC of the patients. We found a significant relationship between the PCC FC and performance in trail making A, Rey memory test, normalized brain volume, and normalized white matter lesion load. On the other hand, the FC IPS was significantly correlated with performance in the trail making B test. The results suggest that resting-state FC might have the potential to be translated into a clinical biomarker that is sensitive to disease progression.**

***Keywords - small vessel disease, CADASIL, fMRI, independent component analysis, seed-based correlational analysis, resting-state networks, functional connectivity.**

1. Introduction

In people aged over 65 years old, small vessel disease (SVD) is one of the most important contributors to cognitive decline and functional loss, contributing to up to 45% of dementia, and is responsible roughly for about 20% of stroke globally [1]. Presently, several investigations demonstrated that cerebral SVD is highly correlated with neurological dysfunctions [2]. Anatomically, small vessels include the vascular structures with a diameter up to 500µm located in the brain parenchyma and subarachnoid space [3]. The term SVD has a broad meaning and refers to brain parenchymal damage. Rincon et al [4] define SVD as a *"syndrome of clinical, cognitive, neuroimaging, and neuropathological findings"* considered to emerge from intracerebral vessel pathology. The SVD types most frequently encountered in clinical practice are arteriosclerosis or age-related SVD and cerebral amyloid angiopathy. SVD can arise due to vascular risk factors – sporadic SVD – or by genetic disorders – cerebral autosomal dominant arteriopathy with subcortical infarcts and leukoencephalopathy (CADASIL). [4].

The effects of cerebral SVD are mainly injuries located in subcortical areas, specifically lacunar infarcts, white matter lesions, and haemorrhages. These SVD consequences can be observed by neuroimaging techniques, whereas small vessels are not easily imaged. Thereby, the SVD expression is frequently applied to describe the brain injuries assessed through neuroimaging methods, i.e. the pathological consequences of SVD, instead of the underlying small vessel disturbances. Progress in understanding and managing SVD has been relatively slow due to the lack of a good disease marker that is able to track disease stages [6].

fMRI has expanded significantly since it was first performed in the mid-1990s. It exhibits valuable features such as non-invasiveness, safeness, good spatial resolution and relatively good temporal resolution [7]. The most common method towards fMRI is based on a phenomenon known as blood oxygenation level dependent (BOLD). Resting-state fMRI analyses spontaneous fluctuations in the BOLD signal without requiring subjects to perform a task. The incentive to study spontaneous activity arises from the realization that the brain at rest has revealed highly metabolic. Nowadays, there is an expansion in the application of resting-state fMRI to examine functional connectivity (FC), which refers to how different areas of the brain exhibit similar temporal patterns [9]. Resting-state fMRI investigations allowed the identification of roughly 20 so-called resting-state networks (RSNs), which are reproducible across individuals and methods. The most common RSNs are depicted in Figure 1.1 [10].

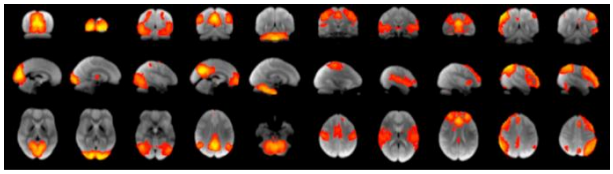

Figure 1.1: 10 RSNs reported by Smith et al ([10]). From left to right: visual medial, visual occipital, visual lateral area; default mode network; cerebellum; sensorimotor area; auditory area; executive control; right frontoparietal, left frontoparietal.

The most widely studied is the default mode network (DMN), which is a task-negative network - active at rest and deactivated in task-based fMRI experiments. Conversely, task-positive networks include visual, auditory, executive control, sensorimotor, frontoparietal, salience, dorsal-attention and cerebellum networks. The DMN and task-positive networks are highly associated – with the activity of the former decreasing with the activation of the latter [9]. Alterations in these networks can be observed in different situations such as ageing - most findings demonstrate a reduction in DMN FC [11]; From a clinical perspective, these connectivity networks are of huge importance since they can serve as potential disease markers by reflecting functional activity [10].

Up to date, there are only a small number of studies and reports on patients with SVD who underwent resting-state fMRI; focusing on early SVD [13] and CADASIL [14]. Related studies were also considered throughout this work, which employed resting-state fMRI on patients with vascular cognitive impairment (no dementia) [11], and subcortical vascular mild cognitive impairment [12] [15]. These studies were included since the underlying pathophysiology mechanisms of the different conditions are to some extent related to SVD. They differ on the data acquisition, pre-processing used and the type of method implemented in the analysis. The most important conclusions that can be withdrawn from these investigations are: Schaefer et al [13] demonstrated reduced FC in frontoparietal networks in patients with early SVD, which is closely associated to white matter lesions and neuropsychological disturbances. These results are in accordance with the findings of Yi et al [15]. In addition, Sun et al [11] found impaired FC between the anterior and posterior parts of DMN in patients with a vascular etiology similar to subcortical vascular mild cognitive impairment.

The main objective of this work is to investigate alterations of intrinsic FC in sporadic SVD and CADASIL, based on the analysis of resting-state fMRI data, through comparison with healthy controls and through the association with demographic, neuropsychological and structural imaging measures. In order to accomplish this objective, the following specific objectives were defined: (i) To, pre-process the acquired structural and functional images from both patients and healthy controls, using well-established methodologies; (ii) To analyse intrinsic functional connectivity and assess differences between groups, using two different methods applied to the resting-state fMRI data: ICA and seed-based analysis. (iii) To investigate the relationship between intrinsic functional connectivity measures and relevant quantitative parameters of each participant, namely: demographical (age), neuropsychological (cognitive tests), and structural (lesion and brain volume), using multiple linear regression and a stepwise model to assess which measures best explain the mean connectivity encountered. The results from this study are expected to provide an added value for the possibility of introducing changes in functional connectivity as an efficient biomarker that helps obtaining a fast and reliable diagnostic. In fact, since SVD is a complex and heterogeneous disease, the inclusion of a biomarker might work as an important complement to increase confidence in the diagnosis. Furthermore, this work may aware the scientific community to further investigate the usage of resting-state BOLD images to assess disturbances in different types of dementia.

2. Materials and Methods

2.1. Data description

Data used were obtained on a 3T Siemens Verio MRI system using a 12-channel RF coil at Hospital da Luz between 2015 and 2017, in the scope of the research project NEUROPHYSIM. The participants included are 11 sporadic SVD (S-SVD) patients, 6 CADASIL patients, and 8 healthy controls.

The neuropsychological evaluation of the patients consisted of a comprehensive battery of cognitive tests that evaluate four relevant cognitive domains, namely: (i) Trailmaking test part A – measures processing speed, i.e., visual attention combined with information processing; (ii) Trailmaking test part B – measures executive function as well as working memory [13]; (iii) Wechsler Adult Intelligence Scale (WAIS-III), specifically the digit span sub-test – assesses attention and working memory [14]; (iv) Rey-osterrieth complex figure memory sub-test – measures long-term/non-verbal memory and some features of executive function [15].

The data acquired for all subjects were a T1-weighted and T2-weighted structural image as well as resting-state BOLD fMRI data. The T1-weighted images were collected using an MPRAGE sequence with parameters $TE = 2.26\,ms,\ TI = 900\,ms,\ TR = 2250\,ms$ and flip angle of 9º. These images covered the from the whole-brain with a voxel resolution of $1{\times}1{\times}1\ mm^3$ and are represented by a matrix of size $240{\times}256{\times}144$ and thus, have a FOV of $240{\times}256{\times}144\ mm^3$.

The T2-weighted images were collected using a fluid attenuation and inversion recovery (FLAIR) sequence, with parameters $TE = 97$ ms, $TI = 2500\,ms$, $TR = 8500\,ms$ and flip angle of 150º. The voxel resolution of these images are $0.7{\times}0.7{\times}3.3\ mm^3$ and have a matrix size of $256{\times}320{\times}47$, consequently the FOV is $179{\times}224{\times}155\ mm^3$.

During the resting-state fMRI acquisition, the subjects were instructed to keep their eyes closed and restrain from moving as much as possible. A gradient-echo EPI sequence was used to acquire the functional images with parameters $TE = 50\,ms$, $TR = 2500\,ms$, voxel

resolution of 3.5×3.5×3.0 mm^3, matrix = 64×64×40, hence with a FOV of 224×224×120 mm^3, duration= 5 minutes.

2.2. Imaging Analysis

2.2.1. Pre-processing

All image analyses were performed using FSL tools (https://fsl.fmrib.ox.ac.uk/fsl).

Some pre-processing steps were first performed on the T1-weighted structural images. Firstly, non-brain components are extracted from structural images using FSL's Brain Extraction Tool (BET). These images were used to extract the structural measures that will be included in the statistical analysis: normalized brain volume (nBV) and normalized white matter lesion load (nWMLL). The nBV was estimated based on the T1-weighted images using FSL's tool SIENAX (https://fsl.fmrib.ox.ac.uk/fsl/fslwiki/SIENA). The total volume of brain is estimated, and normalized with respect to each individual's skull size. For the computation of nWMLL, the white matter hyperintensities (WMH) were identified and segmented manually on the T2-weighted images. The respective volume was then computed and normalized by the respective brain volume of each individual.

For each BOLD fMRI dataset, the following pre-processing steps were executed using FSL's FEAT tool (https://fsl.fmrib.ox.ac.uk/fsl/fslwiki/FEAT/): (i) non-brain removal using BET; (ii) motion correction to attenuate the effect of head motion by aligning all acquired volumes with respect to a reference volume using rigid body transformations (MCFLIRT tool); (iii) spatial smoothing using a Gaussian kernel with 5 mm FWHM is conducted individually in each volume of the fMRI data set; (iv) high-pass temporal filtering with cut-off = 40 TRs = 100s which is the recommended value for resting-state fMRI data [16]. Ultimately, ICA denoising was applied using FSL's tool FIX (https://fsl.fmrib.ox.ac.uk/fsl/fslwiki/FIX/). This tool classifies ICA components into quality signal vs noise components, by application of a training dataset.

2.2.2. Registration

The pre-processed fMRI data underwent registration to the T1-weighted image of the respective subject, as well as to the MNI standard space, also using FSL's FEAT tool. The registration is a 2-stage process: the reference functional image is registered to the T1-weighted structural image through the boundary-based registration (BBR) method (https://fsl.fmrib.ox.ac.uk/fsl/fslwiki/FLIRT_BBR). Then the high resolution structural image is normalized to a standard space (MNI152, T1-weighted, 2×2×2 mm^3) using a non-linear registration tool, FNIRT (https://fsl.fmrib.ox.ac.uk/fsl/fslwiki/FNIRT/). Finally, the two transformations are combined, taking the low-resolution fMRI image into the standard space.

2.2.3. FC analysis

Spatial ICA was performed on the group data using FSL's MELODIC software implementing probabilistic ICA(https://fsl.fmrib.ox.ac.uk/fsl/fslwiki/MELODIC/). The methodology used to perform group inferences was multi-session temporal concatenation. After multi-subject ICA analysis was conducted, FSL's dual regression(https://fsl.fmrib.ox.ac.uk/fsl/fslwiki/DualRegression) was performed to assess FC differences across the 3 groups. Finally, a group analysis is conducted by entering the participants' individual IC spatial maps in a general linear model framework, using an appropriate design matrix and corresponding contrasts (https://fsl.fmrib.ox.ac.uk/fsl/fslwiki/GLM) as exemplified in Figure 2.1.

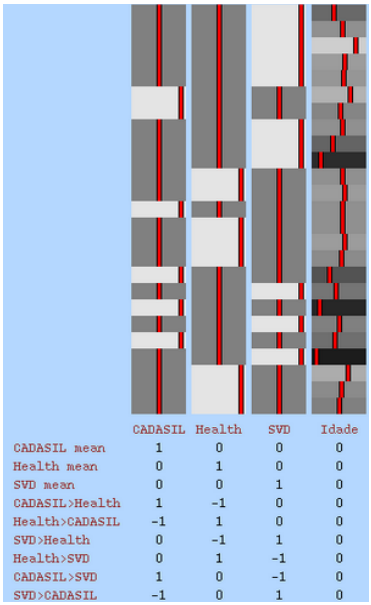

Figure 2.1: design matrix used for the analyses with the 4 explanatory variables: CADASIL, Healthy, S-SVD group and age as well as 9 t-test contrasts. Note: SVD explanatory variable refers to S-SVD.

For the seed-based analysis, three seeds were defined in MNI space, based on previous literature[17]: posterior cingulate cortex (PCC) (MNI coordinates: -6, -58, 28), supplementary motor area (SMA) (MNI coordinates: -2, 10, 48) and intraparietal sulcus (IPS) (MNI coordinates: 26, -58, 48). For each seed, a ROI was then defined as a sphere of radius of 5 mm. A first-level analysis was carried out in FSL's tool FEAT (https://fsl.fmrib.ox.ac.uk/fsl/fslwiki/FEAT.), using three explanatory variables corresponding to the average BOLD fMRI time courses within the three seed ROIs; 3 contrasts of parameter estimates (COPEs) were defined,

one for each EV. The output from the single-subject analysis was fed into a higher-level analysis using a mixed-effects model as implemented in FSL's tool FLAME. The GLM defined in this group analysis is the same as the one presented in Figure 2.1.

2.3. Statistical analysis

A statistical analysis of the mean FC measured in each patient using resting-state fMRI was performed in order to investigate its relationship with relevant demographic, neuropsychological and brain structure measures. For this purpose, a multiple linear regression was conducted using the mean FC values as outcome measures and the other quantitative measures as explanatory variables. From the ICA analysis, the mean value was extracted from the individual IC Z-map of interest across the voxels exhibiting differences between patients and controls. Secondly, from the seed-based analysis, the mean value was extracted from the individual COPE map obtained for each seed (PCC, SMA and IPS), across the voxels exhibiting signal changes significantly associated with the respective seed. The quantitative measures that were considered for each patient are: age, structural brain measures (nBV, and nWMLL), and neuropsychological measures from different cognitive domains (Trailmaking A, Trailmaking B, WAIS-III: digit span, and Rey memory sub-tests). A stepwise model was used to select the ensemble of covariates that best explain the mean connectivity observed. All statistical analyses were performed in R statistics software [18].

3. Results

3.1. Independent Component Analysis

The independent components (ICs) obtained with the group analysis that correspond to well-established RSNs, according to Smith et al, are represented in Figure 3.1 However, there is one RSN missing from this analysis when compared with the 10 RSNs maps from Smith et al, specifically, the right frontoparietal RSN. The only RSN IC exhibiting significant group differences was the sensorimotor RSN (IC 12) This RSN includes the precentral gyrus, post central gyrus, supplementary motor area and some parietal cortex regions. Specifically, within this RSN, a decrease in FC was found in the S-SVD group compared with the control group (Figure 3.2).

The anatomical structures where group differences were more pronounced and consequently, must be highlighted are: (i) the postcentral gyrus, known as sensory strip, comprises the primary somatosensory cortex which is an elementary receptor of somatic sensation from thalamus.[19]; (ii) the precentral gyrus, denominated motor strip, includes the primary motor cortex which is responsible for the execution and control of voluntary movements; (iii) the superior parietal lobule which is connected to the postcentral gyrus and is involved in attention and visuospatial tasks[20]; (iv) the precuneus cortex which is responsible for several cognitive processes. It includes functions such as integration of environmental information, episodic memory, self-consciousness, mental imaginary and visuospatial processing[21].

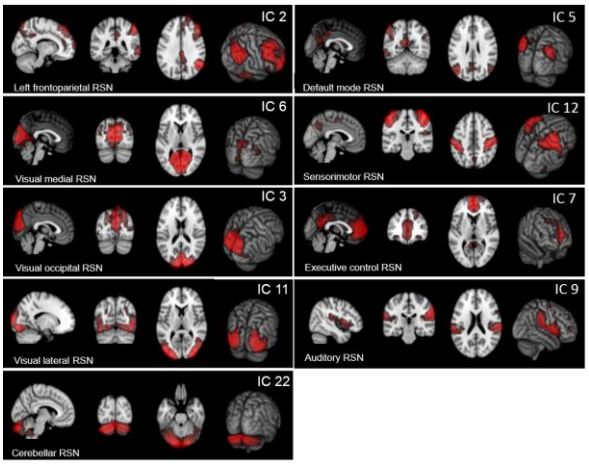

Figure 3.1: RSNs obtained from the group ICA analysis. The RSNs are shown as the Z-maps of the identified ICs (3<Z<9); one representative slice at each orientation is shown, as well as a 3D representation of the brain surface.

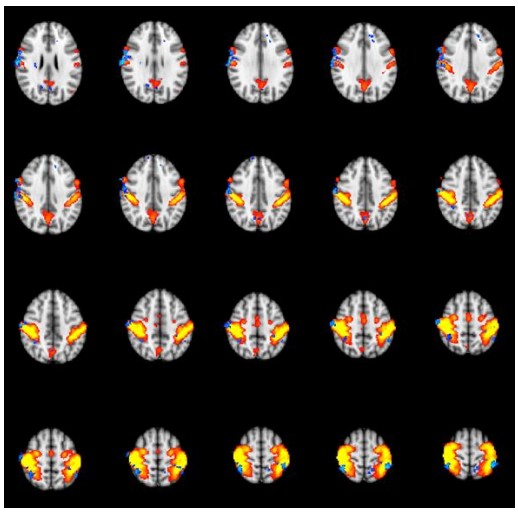

Figure 3.2: Map of significantly decreased FC in the sensorimotor RSN between S-SVD patients and controls (blue to light blue, 0.95 < corrected p-value < 1.00), overlaid on the Z map of the respective IC (red to yellow, 3< Z < 9); 20 representative axial slices are shown.

Regarding the network mean FC analysis, the results of the multiple linear regression, and respective step model analysis for the mean connectivity of the somatosensory RSN (IC12) are presented in Table 3.1. The overall model including all explanatory variables can predict FC of IC12 significantly (p=0,05), explaining 54,7% of its variance, although only age exhibits a significant

negative relationship (p=0,045). Nevertheless, the stepwise model analysis revealed that the best model includes only the following explanatory variables: age, nBV and WAIS-III digit span neuropsychological sub-test (p=0,0007), explaining 65,3% of variance in FC of IC12. This is found to decrease with age, while it increases with brain volume and with working memory and attention performance.

Table 3-1: Multiple linear regression and stepwise model analysis for the mean connectivity from IC12 as dependent variable. β=parameter estimate; SE=standard error; R-squared = adjusted coefficient of variation. The p-values presented correspond to the coefficients of the individual regressors and to the overall significance of the model.

		β	SE	p-value
Multiple linear regression				
Age		-0,027	0,011	**0,045**
nWMLL		1,963	7,099	0,789
nBV		0,004	0,002	0,097
Trailmaking A		0,005	0,005	0,341
Trailmaking B		-0,002	0,002	0,37
WAIS-III: digit span sub-test		0,023	0,032	0,491
Rey: memory sub-test		-0,015	0,022	0,528
p-value: overall significance	**0,05**			
multiple R-squared	0,774			
adjusted R-squared	0,547			
Stepwise model				
Age		-0,024	0,009	**0,016**
nBV		0,003	0,001	0,057
WAIS-III: digit span sub-test		0,029	0,013	**0,049**
p-value: overall significance	**0,0007**			
multiple R-squared	0,718			
adjusted R-squared	0,653			

In this way, the reduced FC verified in the sensorimotor RSN can be explained by mechanisms of ageing and brain atrophy, and are associated with cognitive performance measured by the WAIS-III digit span neuropsychological sub-test which include the following domains: attention and working memory.

3.2. Seed-based analysis

Concerning model-based analysis, three seeds were selected to investigate their affected connections with other brain regions.

3.2.1. Whole-brain FC analysis

The between-group differences in resting-state FC using the PCC as a seed are described in table 3.2 and the respective maps are shown in figure 3.3. Compared with the healthy control group, S-SVD patients demonstrated increased FC in the left inferior and superior parietal lobule. Regarding differences between the two patients' populations, i.e. CADASIL vs S-SVD, CADASIL subjects revealed increased FC in the right middle temporal gyrus, left temporal lobe and left postcentral gyrus. Conversely, S-SVD patients exhibited increased connectivity in the left inferior parietal lobule and the right thalamus. Notably, the left inferior parietal lobule is a region of increased activity in the S-SVD population when compared with both healthy and CADASIL groups.

Table 3-2: Characteristics of the clusters showing significant group differences in the FC of PCC.

	Cluster index	Number of cluster voxels	Peak MNI coordinate (mm)			Peak MNI coordinate region
			x	y	z	
S-SVD>Healthy	1	1347	-38	-70	28	Left superior and inferior parietal lobule
	1	453	66	-32	0	Right middle temporal gyrus
	2	664	-54	18	-8	Left temporal lobe
CADASIL>S-SVD	3	4538	-6	-48	70	Left postcentral gyrus
	1	473	-42	-74	28	Left inferior parietal lobule
S-SVD>CADASIL	2	513	16	-28	-14	Right Thalamus

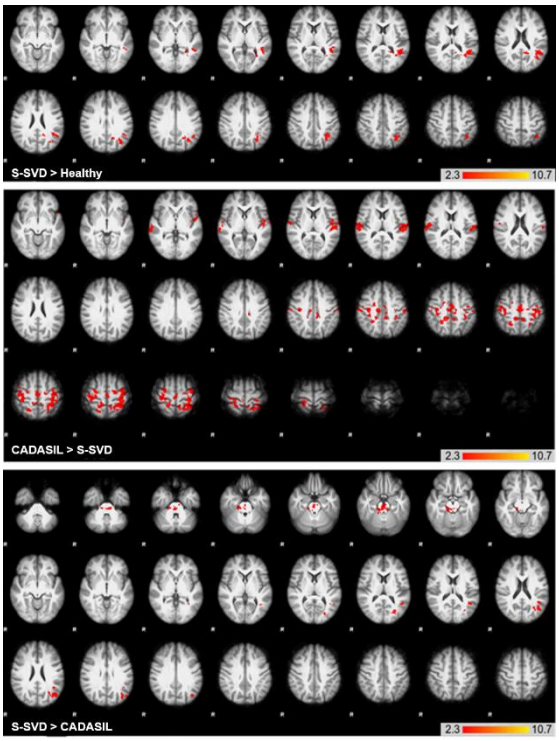

Figure 3.3: maps showing significant group differences in the FC of PCC. The MNI images are overlaid by z-maps of specific contrasts (red to yellow, 2.3 < Z < 10.7) such as: S-SVD>Healthy (top image); CADASIL>S-SVD (middle image); S-SVD>CADASIL (bottom image). Representative axial slices are shown.

The between-group differences in resting-state FC with the SMA are described in Table 3.3 and the maps are depicted in Figure 3.4. When compared with controls, both S-SVD and CADASIL patients had reduced SMA FC in multiple brain areas. Interestingly, the affected brain regions were different in the two patient groups, and indeed both greater and weaker SMA FC was found in one group relative to the other.

The CADASIL group revealed decreased FC in the right and left thalamus as well as in the cerebellum, when compared with controls. Concerning S-SVD patients compared with controls, they exhibited reduced FC in the right frontal lobe, left inferior frontal gyrus, precuneus cortex and both right and left occipital lobes. Regarding the comparison between both groups of patients, besides the decreased FC in the right occipital

lobe, the S-SVD population revealed weaker FC in the left insula. Conversely, the S-SVD group showed increased FC in the right putamen compared to CADASIL.

Table 3-3: Characteristics of the clusters showing significant group differences in the FC of SMA.

	Cluster index	Number of cluster voxels	Peak MNI coordinate (mm)			Peak MNI coordinate region
			x	y	z	
	1	908	6	-2	10	Right thalamus
	2	1237	-6	-20	8	Left thalamus
Healthy>CADASIL	3	1815	0	-42	-34	cerebellum
	1	362	44	56	10	Right frontal lobe
	2	535	-52	40	-4	Left inferior frontal gyrus
	3	558	2	-62	12	Precuneus cortex
	4	691	16	-96	28	Right occipital lobe
Healthy>S-SVD	5	1820	-6	-100	-8	Left occipital lobe
	1	340	-44	18	-6	Left insula
CADASIL>S-SVD	2	2880	6	-100	14	Right occipital lobe
S-SVD>CADASIL	1	382	22	2	-4	Right putamen

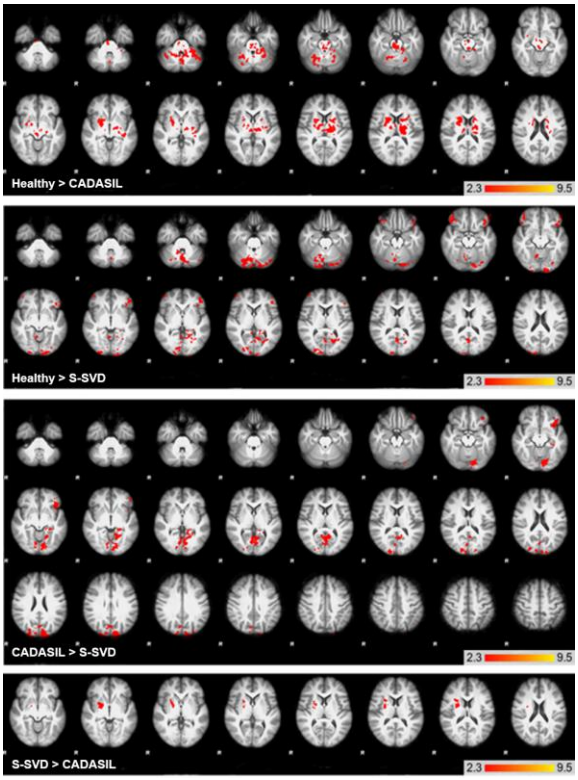

Figure 3.4: maps showing significant group differences in the FC of SMA. The MNI images are overlaid by z-maps of specific contrasts (red to yellow, $2.3 < Z < 9.5$) such as: Healthy>CADASIL (top image); Healthy > S-SVD (first middle image); CADASIL> S-SVD (second middle image); S-SVD > CADASIL (bottom image). Representative axial slices are shown.

The between-group differences in resting-state FC using the IPS as a ROI are specified in table 3.4 and the corresponding maps are presented in figure 3.5.

Table 3-4: Characteristics of the clusters showing significant group differences in the FC of IPS.

	Cluster index	Number of cluster voxels	Peak MNI coordinate (mm)			Peak MNI coordinate region
			x	y	z	
	1	615	56	-36	0	Right middle temporal gyrus
	2	788	4	-58	64	Precuneus cortex
	3	1823	44	-12	66	Right precentral gyrus
	4	2037	-14	-54	74	Left parietal lobe
Healthy>CADASIL	5	8482	14	-84	50	Right occipital lobe
Healthy>S-SVD	1	26139	-6	-86	44	Left occipital lobe
S-SVD>Healthy	1	326	-48	-64	50	Left parietal lobe

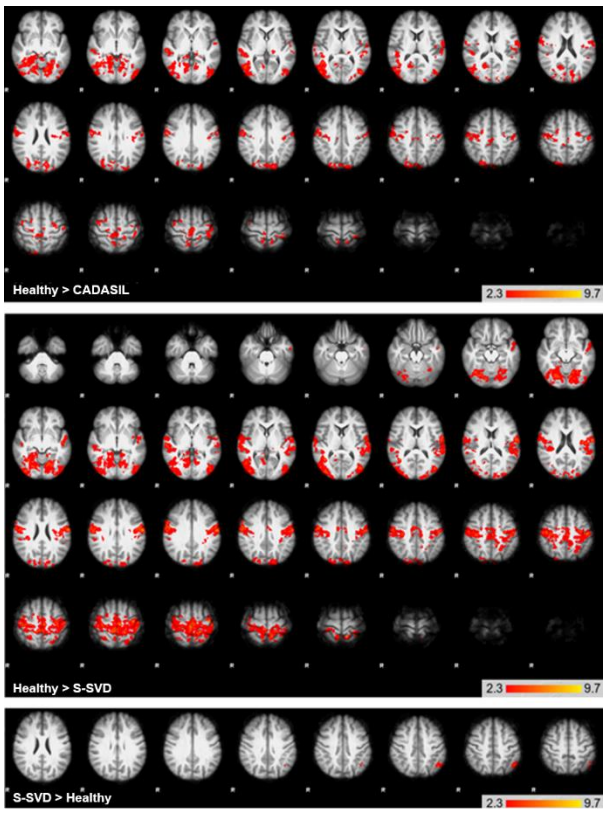

Figure 3.5: maps showing significant group differences in the FC of IPS. The MNI images are overlaid by z-maps of specific contrasts (red to yellow, $2.3 < Z < 9.7$) such as: Healthy>CADASIL (top image); Healthy > S-SVD (middle image); S-SVD > Healthy (bottom image). Representative axial slices are shown.

In this case, compared with controls, both S-SVD and CADASIL patients revealed decreased FC in an extended part of the IPS network. For the CADASIL patients, reduced FC was found in the right middle temporal gyrus, precuneus cortex, right precentral gyrus, left parietal lobe and right occipital lobe. As observed in the previous section, the activity of the precuneus cortex is affected within the groups of patients. Additionally, in accordance with the results from the whole-brain SMA connectivity, the S-SVD group showed reduced FC in the left occipital lobe. On the other hand, the left parietal lobe revealed increased FC which agrees with the findings of the whole-brain PCC connectivity.

3.2.2. Network mean FC analysis

The results for the PCC connectivity using multiple linear regression and stepwise model analyses are presented in Table 3.5. Looking at the overall p-value obtained from the multiple linear regression model ($p = 0{,}03$), one can conclude that the covariates are overall significantly associated with the PCC mean connectivity, explaining 61,2% of the mean FC variance. The stepwise algorithm, however, revealed that the best model includes specifically the following explanatory variables: nWMLL, nBV, trailmaking A and Rey memory neuropsychological sub-tests. This latter model has a p-value of 0,001 and explains 71,7% of variance.

Table 3-5: Multiple linear regression and stepwise model analyses for the PCC mean FC as dependent variable. β=parameter estimate; SE=standard error; R-squared = adjusted coefficient of variation. The p-values presented correspond to the coefficients of the individual regressors and to the overall significance of the model.

		β	SE	p-value
Multiple linear regression				
Age		6,32E-05	2,471E-03	0,98
nWMLL		2,477	1,538	0,146
nBV		-6,036E-04	4,121E-04	0,181
Trailmaking A		-1,284E-03	1,169E-03	0,304
Trailmaking B		2,957E-06	4,546E-04	0,995
WAIS-III: digit span sub-test		2,416E-04	7,030E-03	0,973
Rey: memory sub-test		5,344E-03	4,951E-03	0,311
p-value: overall significance	**0,03**			
multiple R-squared	0,806			
adjusted R-squared	0,612			
Stepwise model				
nWMLL		2,523	0,863	**0,014**
nBV		-6E-04	3E-04	0,062
Trailmaking A		-1E-03	7E-04	0,081
Rey: memory sub-test		5E-03	3E-03	0,078
p-value: overall significance	**0,001**			
multiple R-squared	0,806			
adjusted R-squared	0,717			

The results of the statistical analysis for the SMA connectivity are exhibited in Table 3.6.

Table 3-6: Multiple linear regression and stepwise model analyses for the SMA mean FC as dependent variable. β=parameter estimate; SE=standard error; R-squared = adjusted coefficient of variation. The p-values presented correspond to the coefficients of the individual regressors and to the overall significance of the model.

		β	SE	p-value
Multiple linear regression				
Age		0,004	0,005	0,412
nWMLL		0,285	3,029	0,927
nBV		-0,0005	0,0008	0,55
Trailmaking A		-0,0009	0,002	0,677
Trailmaking B		0,0003	0,0009	0,739
WAIS-III: digit span sub-test		-0,004	0,014	0,792
Rey: memory sub-test		0,013	0,009	0,235
p-value: overall significance	0,595			
multiple R-squared	0,456			
adjusted R-squared	-0,087			
Stepwise model				
Age		0,005	0,003	0,163
Rey: memory sub-test		0,007	0,004	0,077
p-value: overall significance	0,07			
multiple R-squared	0,398			
adjusted R-squared	0,259			

Looking at table 3.6, the overall p-value from both models is not significant, nor does the best model obtained by the stepwise algorithm reach significance. Thus, it is not possible to state that the covariates investigated here are related with the SMA mean FC. Finally, the results of the multiple linear regression and stepwise model in the case of IPS connectivity are in Table 3.7. Looking at table 3.10, the stepwise algorithm revealed a model that significantly explained the IPS mean FC results, which is based only on the performance in the trailmaking B test. This neuropsychological test evaluates executive function and working memory.

Table 3-7: Multiple linear regression and stepwise model analyses for the IPS mean FC as dependent variable. β=parameter estimate; SE=standard error; R-squared = adjusted coefficient of variation. The p-values presented correspond to the coefficients of the individual regressors and to the overall significance of the model.

		β	SE	p-value
Multiple linear regression				
Age		0,006	0,005	0,254
nWMLL		0,658	3,167	0,841
nBV		0,0008	0,0008	0,366
Trailmaking A		0,0005	0,002	0,828
Trailmaking B		-0,001	0,0009	0,136
WAIS-III: digit span sub-test		-0,012	0,014	0,424
Rey: memory sub-test		-0,0004	0,01	0,969
p-value: overall significance	0,430			
multiple R-squared	0,532			
adjusted R-squared	0,064			
Stepwise model				
Trailmaking B		-0,0007	0,0003	**0,041**
p-value: overall significance	**0,041**			
multiple R-squared	0,249			
adjusted R-squared	0,199			

Finally, instead of defining the mean FC as the dependent variable of the multiple linear regression and stepwise model analysis, the cognitive tests were defined as the response variable and the same statistical procedure was conducted. The purpose of this analysis was to evaluate the predictive power of FC, compared to those of structural brain measures or age, in predicting the patients' cognitive performance. For this purpose, the covariates included in the analysis were age, nBV, nWMLL, and the mean FC of PCC, SMA and IPS, and the response variables are the four different cognitive tests. The models obtained using the stepwise model analysis for each test are displayed in Table 3.8.

Table 3-8: stepwise model with the neuropsychological tests as dependent variables. β=parameter estimate; SE=standard error; R-squared = adjusted coefficient of variation. The p-values presented correspond to the individual coefficients and the overall significance of the model.

		β	SE	p-value
Trailmaking A				
Age		1,106	0,657	0,117
nBV		-0,136	0,108	0,232
PCC mean connectivity		-149,954	67,556	**0,046**
p-value: overall significance	0,07			
Trailmaking B				
Age		5	2,073	**0,043**
PCC mean connectivity		-361,507	210,395	0,111
IPS mean connectivity		-354,273	132,716	**0,02**
p-value: overall significance	**0,03**			
WAIS-III: digit span sub-test				
nBV		0,045	0,02	**0,042**
PCC mean connectivity		43,818	14,117	**0,008**
p-value: overall significance	**0,04**			
Rey: memory sub-test				
nWMLL		-237,022	65,245	**0,003**
nBV		0,042	0,02	0,059
PCC mean connectivity		51,686	15,686	**0,005**
p-value: overall significance	**0,003**			

It is possible to observe that the trailmaking test A did not exhibit significant results (p-value=0,07). Nonetheless, the remaining cognitive tests revealed significant correlations with a specific arrangement of covariates. The reaction times of the trailmaking test B can be best explained by age, PCC and IPS mean FC. Regarding the WAIS-III digit span sub-test, the scores can be explained by nBV and PCC mean FC. Finally, the covariates explaining the results from the rey memory sub-test are both structural measures together with the PCC mean FC. Remarkably, the PCC mean FC consistently belongs to the ensemble of covariates that explain the response variables, i.e. the outcomes from the battery of cognitive tests.

4. Conclusions

The primary goal of this work was to demonstrate changes in the resting-state FC in patients with S-SVD and CADASIL compared with a healthy control group. This goal was accomplished; however, it should be further validated by including more subjects equally distributed among the groups.

From the sensorimotor RSN mean FC analysis, one can conclude that ageing influences the mean FC of this network. Previous studies have reported reduced connectivity within RSNs related to normal ageing. Typically, cognitive decline accompanies healthy ageing [22]. Differentiate whether cognitive decline is purely due to advanced ageing or is involved in the underlying vascular disease is increasingly important. Besides age, the covariates that best explain the mean FC from the sensorimotor RSN are the nBV and the WAIS-III digit span sub-test. The latter covariate is responsible for evaluating working memory and attention. Notably, regarding the whole-brain FC analysis of the sensorimotor RSN, the S-SVD population showed decreased connectivity in brain areas responsible for episodic memory (precuneus cortex) and attention (superior parietal lobule) when compared with the healthy control group. The SVD is also characterized by structural alterations, such as brain atrophy and white matter lesion load, that play a role in cognitive decline as well [23]. In fact, a recent investigation concluded that lesion volume and abnormal brain volume influence the speed of information processing (measured by trailmaking A test) as well as contributing to executive dysfunction (measured by trailmaking B test)[24].

In terms of whole-brain PCC FC analysis, the increased FC verified in S-SVD subjects in the left superior parietal lobule had already been reported in a previous study of patients with vascular cognitive impairment without dementia [25]. The CADASIL group showed higher FC than S-SVD patients in some temporal structures, a result that had been published using as a study sample, patients with subcortical vascular cognitive impairment. The overall enhanced connectivity of the PCC in SVD patients might be explained as a compensatory plasticity mechanism that arises due to the presence of lesions obstructing the corresponding neural networks [26].

Regarding the whole-brain SMA FC analysis, the decreased FC observed in the cerebellum in the CADASIL group, when compared with the healthy population, might be explained since the chromosome responsible for CADASIL encodes other autosomal dominant disease, called episodic hereditary cerebellar ataxia that translates into cerebellum degenerative disorders[27]. Therefore, the reduction in cerebellum activity within the CADASIL subjects might be due to the fact that both disorders are intimately related. On the other hand, in relation to the healthy group, S-SVD showed reduced FC in the precuneus cortex. These finding is in accordance with a previous study in patients with subcortical vascular cognitive impairment[28]. Additionally, the decreased FC in the occipital lobes may be caused due to the preferential accumulation of cerebral microbleeds in these areas in patients with S-SVD (cerebral amyloid angiopathy)[29]. The reduced FC verified within the frontal lobes might had emerged due to atrophy in this anterior brain area [30] since typically, reduced brain volume is detected in patients with SVD. Importantly, it is also hypothesized a dissociation of the frontal-subcortical pathways as a mechanism that leads to loss of cognition commonly observed in this diseased group[25].

In relation to the whole-brain IPS FC analysis, the decreased FC exhibited in the middle temporal gyrus witihin the CADASIL group, compared to the healthy subjects, had been reported in a previous study using a study sample with clinical similarities to SVD [25]. Regarding the right precentral gyrus, an investigation in CADASIL patients was carried out that demonstrated cortical thickness in this structure which could be the cause for the reduced FC [31]. Additionally, within the CADASIL population, one of the most damaged area by white matter lesions is the left parietal lobe whereas the occipital lobe are changeably affected[32]. This finding could explain the reduced FC found in those areas.

Concerning the PCC mean FC analysis, the nWMLL is one of the covariates that best explains the model. A previous study on PCC connectivity in patients with vascular cognitive impairment no dementia revealed that FC might be affected by white matter lesions. In this way, the structural connectivity of the DMN, and hence its functional integrity, would be disrupted [25]. Interestingly, a recent study reported that the brain atrophy of the hippocampus as well as its structural and functional disconnection with the rest of the DMN might

be the cause of mild memory impairment found in the SVD population [33]. Importantly, from the statistical analysis, one can deduce that the mean FC correlates with the Rey memory sub-test which assesses long-term memory. Additionally, FC is also associated with trailmaking A test, i.e. with information processing speed. Since white matter tracts are responsible for sustaining an efficient transmission of neural signals across different pathways, when they are damaged, cause an overall slowing of cognitive processing.

Looking at the SMA mean FC analysis, there is no significant result from both statistical analysis. However, a recent study in early SVD using network centrality analysis, revealed that the lower the centrality in sensorimotor areas, the slower was the reaction time in the trailmaking A test[34]. It is possible that our study, either lacked sensitivity to detect a similar effect, or did not investigate the relevant network measure in this case, namely its centrality.

With regard to the IPS mean FC analysis, the trailmaking B was the covariate that best explained the IPS mean FC of the diseased population. As it has been reported by previous studies, the superior parietal cortex, which is functionally connected to the IPS, is involved in the coordination of information in working memory[35]. As well as processing speed, executive function is typically impaired in SVD patients [3].

Finally, from the neuropsychological performance analysis, one can observe that the PCC mean connectivity is a covariate involved in each model that best explains the scores from the battery of neuropsychological tests, except for the traimaking A. This finding suggests that the FC of the PCC, i.e., within the DMN, may indeed be a sensitive marker of SVD, that is correlated with performance in a number of cognitive testsBesides the importance to enlarge the study sample, there are some issues that would be interesting to explore in the future: (i) investigate the impact of different fMRI data pre-processing options on the results; (ii) investigate other metrics of FC, such as dynamic FC or graph-theoretical network properties, etc. (iii) terminology and definition of SVD concepts, such as imaging features, image acquisition and analysis vary widely among scientific reports. In this way, an effort should be done in order to standardize important terms. Thus, providing consistency within the scientific community

5. References

[1] Y. Shi and J. M. Wardlaw, "Update on cerebral small vessel disease: a dynamic whole-brain disease," *Bmj*, vol. 1, no. 3, pp. 83–92, 2016.

[2] C. S. Thompson and A. M. Hakim, "Living beyond our physiological means: Small vessel disease of the brain is an expression of a systemic failure in arteriolar function: A unifying hypothesis," *Stroke*, vol. 40, no. 5, pp. 322–331, 2009.

[3] T. G. Issac, S. R. Chandra, R. Christopher, J. Rajeswaran, and M. Philip, "Cerebral small vessel disease clinical, neuropsychological, and radiological phenotypes, histopathological correlates, and described genotypes: A review," *J Geriatr.*, vol. 2015, pp. 1–12, 2015.

[4] F. Rincon and C. B. Wright, "Current pathophysiological concepts in cerebral small vessel disease," *Front. Aging Neurosci.*, vol. 6, no. MAR, pp. 1–8, 2014.

[5] A. Joutel *et al.*, "The ectodomain of the Notch3 receptor accumulates within the cerebrovasculature of CADASIL patients," *J. Clin. Invest.*, vol. 105, no. 5, pp. 597–605, 2000.

[6] A. Charidimou, L. Pantoni, and S. Love, "The concept of sporadic cerebral small vessel disease: A road map on key definitions and current concepts," *Int. J. Stroke*, vol. 11, no. 1, pp. 6–18, 2016.

[7] R. a Poldrack and T. E. Nichols, *Handbook of functional MRI data analysis*, vol. 4. 2011.

[8] R. B.Buxton, *Introduction to Functional Magnetic Resonance Imaging Principles and Techniques*, Second Edi. Cambridge University Press, 2009.

[9] M. D.Fox and M. E. Raichle, "Spontaneous Fluctuations in Brain Activity Observed with Functional Magnetic Resonance Imaging," no. December, 2007.

[10] S. M. Smith *et al.*, "Correspondence of the brain ' s functional architecture during activation and rest," 2009.

[11] J. S. Damoiseaux, C. F. Beckmann, and E. J. S. Arigita, "Reduced resting-state brain activity in the "' default network "' in normal aging," no. August, 2008.

[12] F. Barkhof, S. Haller, and S. A. R. B. Rombouts, "Resting-State Functional MR Imaging : A New Window to the Brain," vol. 272, no. 1, pp. 29–49, 2014.

[13] S. Cavaco *et al.*, "Trail making test: Regression-based norms for the portuguese population," *Arch. Clin. Neuropsychol.*, vol. 28, no. 2, pp. 189–198, 2013.

[14] B. Cullen *et al.*, "Resting state connectivity and cognitive performance in adults with cerebral autosomal-dominant arteriopathy with subcortical infarcts and leukoencephalopathy," *J. Cereb. Blood Flow Metab.*, vol. 36, no. 5, pp. 981–991, 2015.

[15] M.-S. Shin, S.-Y. Park, S.-R. Park, S.-H. Seol, and J.

S. Kwon, “Clinical and empirical applications of the Rey–Osterrieth Complex Figure Test,” *Nat. Protoc.*, vol. 1, no. 2, pp. 892–899, 2006.

[16] J. M. Soares, R. Magalhães, P. S. Moreira, and A. Sousa, “A Hitchhiker ’ s Guide to Functional Magnetic Resonance Imaging,” vol. 10, no. November, pp. 1–35, 2016.

[17] Z. Shehzad *et al.*, “The resting brain: Unconstrained yet reliable,” *Cereb. Cortex*, vol. 19, no. 10, pp. 2209–2229, 2009.

[18] R Core Team, “A language and environment for statistical computing.” Vienna,Austria: R foundation for Statistical Computing, 2014.

[19] C.-S. Wanda G. Webb PhD, “Organization of the Nervous System I,” *Neurol. Speech-Language Pathol. (Sixth Ed.*, 2017.

[20] P. J. Bs. B. Ms. FRCPath, “Prefrontal cortex lesions,” *Clin. Neurosci.*, 2014.

[21] A. E. Cavanna and M. R. Trimble, “The precuneus: A review of its functional anatomy and behavioural correlates,” *Brain*, vol. 129, no. 3, pp. 564–583, 2006.

[22] V. La Corte *et al.*, “Cognitive decline and reorganization of functional connectivity in healthy aging: The pivotal role of the salience network in the prediction of age and cognitive performances,” *Front. Aging Neurosci.*, vol. 8, no. AUG, pp. 1–12, 2016.

[23] A. Nitkunan, S. Lanfranconi, R. A. Charlton, T. R. Barrick, and H. S. Markus, “Brain atrophy and cerebral small vessel disease a prospective follow-up study,” *Stroke*, vol. 42, no. 1, pp. 133–138, 2011.

[24] J. G. Baker, A. J. Williams, C. C. Ionita, P. Lee-Kwen, M. Ching, and R. S. Miletich, “Cerebral small vessel disease: cognition, mood, daily functioning, and imaging findings from a small pilot sample.,” *Dement. Geriatr. Cogn. Dis. Extra*, vol. 2, no. 1, pp. 169–79, 2012.

[25] Y. Sun *et al.*, “Abnormal functional connectivity in patients with vascular cognitive impairment, no dementia: A resting-state functional magnetic resonance imaging study,” *Behav. Brain Res.*, vol. 223, no. 2, pp. 388–394, 2011.

[26] W. Ding *et al.*, “Altered functional connectivity in patients with subcortical vascular cognitive impairment-a resting-state functional magnetic resonance imaging study,” *PLoS One*, vol. 10, no. 9, pp. 1–14, 2015.

[27] C. André, “CADASIL: pathogenesis, clinical and radiological findings and treatment.,” *Arq. Neuropsiquiatr.*, vol. 68, no. 2, pp. 287–299, 2010.

[28] L. Yi *et al.*, “Structural and Functional Changes in Subcortical Vascular Mild Cognitive Impairment: A Combined Voxel-Based Morphometry and Resting-State fMRI Study,” *PLoS One*, vol. 7, no. 9, 2012.

[29] J. M. Wardlaw, C. Smith, and M. Dichgans, “Mechanisms underlying sporadic cerebral small vessel disease : insights from neuroimaging,” *Lancet Neurol.*, vol. 12, no. 5, pp. 70060–7, 2013.

[30] Y. Chen, X. Chen, W. Xiao, V. C. T. Mok, K. S. Wong, and W. K. Tang, “Frontal lobe atrophy is associated with small vessel disease in ischemic stroke patients,” *Clin. Neurol. Neurosurg.*, vol. 111, no. 10, pp. 852–857, 2009.

[31] F. De Guio *et al.*, “In vivo high-resolution 7 tesla MRI shows early and diffuse cortical alterations in CADASIL,” *PLoS One*, vol. 9, no. 8, 2014.

[32] D. Stojanov *et al.*, “Imaging characteristics of cerebral autosomal dominant arteriopathy with subcortical infarcts and leucoencephalopathy (CADASIL).,” *Bosn. J. basic Med. Sci.*, vol. 15, no. 1, pp. 1–8, 2015.

[33] J. M. Papma *et al.*, “The effect of hippocampal function, volume and connectivity on posterior cingulate cortex functioning during episodic memory fMRI in mild cognitive impairment,” *Eur. Radiol.*, pp. 1–9, 2017.

[34] A. Schaefer *et al.*, “Early Small Vessel Disease Affects Frontoparietal and Cerebellar Hubs in Close Correlation with Clinical Symptoms—A Resting-State fMRI Study,” *J. Cereb. Blood Flow Metab.*, vol. 34, no. 7, pp. 1091–1095, 2014.

[35] M. Koenigs, A. K. Barbey, B. R. Postle, and J. Grafman, “Superior parietal cortex is critical for the manipulation of information in working memory,” vol. 29, no. 47, pp. 14980–14986, 2009.